An Integral Equation Method for the Evaluation of Conductor and Dielectric Losses in High-Frequency Interconnects

T. EMILIE VAN DEVENTER, STUDENT MEMBER, IEEE, PISTI B. KATEHI, SENIOR MEMBER, IEEE, AND ANDREAS C. CANGELLARIS, MEMBER, IEEE

Abstract—**An integral equation method is developed to solve for the complex propagation constant in multilayer planar structures with an arbitrary number of strip conductors on different levels. Both dielectric losses in the substrate layers and conductor losses in the strips and ground plane are considered. The Green's function included in the integral equation is derived by using a generalized impedance boundary formulation. The microstrip ohmic losses are evaluated by using an equivalent frequency-dependent impedance surface which is derived by solving for the fields inside the conductors. This impedance surface replaces the conducting strips and takes into account the thickness and skin effect of the strips at high frequencies. The effects of various parameters such as frequency, thickness of the lines, and substrate surface roughness on the complex propagation constant are investigated. Results are presented for single strips, coupled lines, and two-level interconnects. Good agreement with available literature data is shown.**

I. INTRODUCTION

SHIELDED microstrip lines are widely used in microwave integrated circuits, where they perform a great variety of functions. It is therefore very important to have an accurate knowledge of their characteristics, i.e., phase velocity, characteristic impedance, and losses as a function of geometry and frequency. Because dissipative losses impose a major limitation on the performance of microstrip interconnects, passive circuits, and radiating elements, it is of interest to improve loss analysis, whereby effects of substrate and non–perfectly conducting strips can be treated individually. Ohmic losses due to the finite conductivity of the strips constitute the prevalent loss effect at microwave and millimeter-wave frequencies. These have been studied by several authors during the past 50 years but consideration has been limited to lower frequencies and electrically thick strips.

The *incremental inductance rule* derived by Wheeler [1] is the foundation for calculating the surface resistivity of conductive strips. From the knowledge of the resistivity, attenuation due to conductor losses has been evaluated by analytic [2], [3] and numerical [4] differentiation. The perturbation method is also frequently used in quasi-static techniques such as the boundary-element method [5] and the finite-element method [6], as well as in spectral-domain full-wave analyses [7], [8].

These techniques are strictly limited to electrically thick conducting strips; i.e., they assume that the conductors have a thickness much greater than the skin depth at the frequency of interest. The thickness is usually taken into account by a modification of the strip width [4], [9]. However in monolithic microwave and millimeter-wave integrated circuits, where the metallization thickness is of the order of a few μm, the skin effect becomes an important issue. In the past few years, several researchers have studied the above problem using variational formulations [10], [11].

This paper represents an approach which evaluates losses in interconnects printed on multilayer substrates and surrounded by a shielding cavity. The electromagnetic fields are expressed by an integral equation which is solved independently inside the conducting strips and in the surrounding region. The solution for the fields inside the conductors provides the surrounding region with a relation between tangential electric and magnetic fields on the surface of the strips which serves as an additional boundary condition. This boundary condition is satisfied by an equivalent infinitesimally thin impedance surface which then replaces the lossy conducting strips. The fields in the dielectric region, which consists of an arbitrary number of layers, are computed by a method of moments solution of Pocklington's integral equation subject to the newly introduced boundary condition. The present technique is applied to several structures, and a number of parameters are investigated.

II. THEORY

Consider an infinitely long, inhomogeneously filled waveguide with several microstrip lines on different levels in the multilayer configuration shown in Fig. 1. The conductor strips are assumed to have finite conductivity σ and

Manuscript received March 31, 1989; revised July 17, 1989. This work was supported by the U.S. Army Research Office under Contract DAAL03-K-0088(23836-EL) (University of Michigan) and by the Semiconductor Research Corporation under Contract 88-MP-086 (University of Arizona).

T. E. van Deventer and P. B. Katehi are with the Radiation Laboratory, Department of Electrical Engineering and Computer Science, University of Michigan, Ann Arbor, MI 48109-2122.

A. C. Cangellaris is with the Electromagnetics Laboratory, Electrical and Computer Engineering Department, University of Arizona, Tucson, AZ 85721.

IEEE Log Number 8931086.

0018-9480/89/1200-1964$01.00 ©1989 IEEE

thickness t. The conductor thickness is usually small compared to the strip dimensions; however, this need not be the case, especially in monolithic microwave and millimeter-wave integrated circuits on GaAs. Also, in practical circuits the strips are usually at least two widths away from the sidewalls of the waveguide to avoid coupling; therefore losses due to the finite conductivity of these walls are neglected in this derivation. However, the effect of a lossy ground plane is analyzed. Both conducting and dielectric regions are assumed to be nonmagnetic, with free-space permeability μ_0. Dielectric losses are accounted for by assuming a complex permittivity for each layer, which in turn implies that the propagation constant $\gamma \equiv jk_z$ is a complex quantity. In the two-dimensional problem, each microstrip mode propagates rectilinearly along the z direction with a dependence of the form $e^{j(\omega t - k_z z)}$.

The integral equation formulation presented in this section is twofold. First, in the dielectric region, the problem is solved by a rigorous hybrid-mode solution where an integral eigenvalue equation is set up. The Green's function is derived by using an equivalent transmission line for the representation of the fields along the direction normal to the dielectric interfaces. This formulation allows for multiple conductors on different planar levels.

Next, the field behavior inside the conductor is described by a quasi-TEM analysis where the magnetic vector potential is related to the unknown current distribution by a static Green's function. This method allows for the computation of the per-unit-length resistance $R(f)$ and the per-unit-length internal inductance of the strip $L_{in}(f)$ as function of frequency. An equivalent surface impedance is then defined which describes, in a physically equivalent sense, the frequency-dependent field penetration in the lossy strips.

The novelty of this method resides in the application of the boundary condition on the strip where the tangential electric field is related to the finite current on the strip by the surface impedance described above. The resulting general integral equation that accounts for both dielectric and conductor losses is solved numerically by the method of moments.

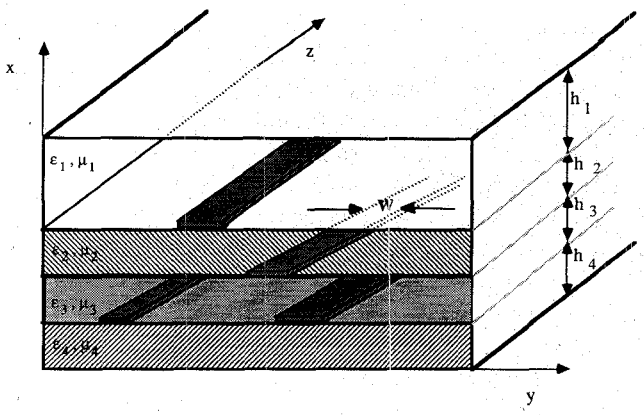

Fig. 1. General shielded microstrip configuration.

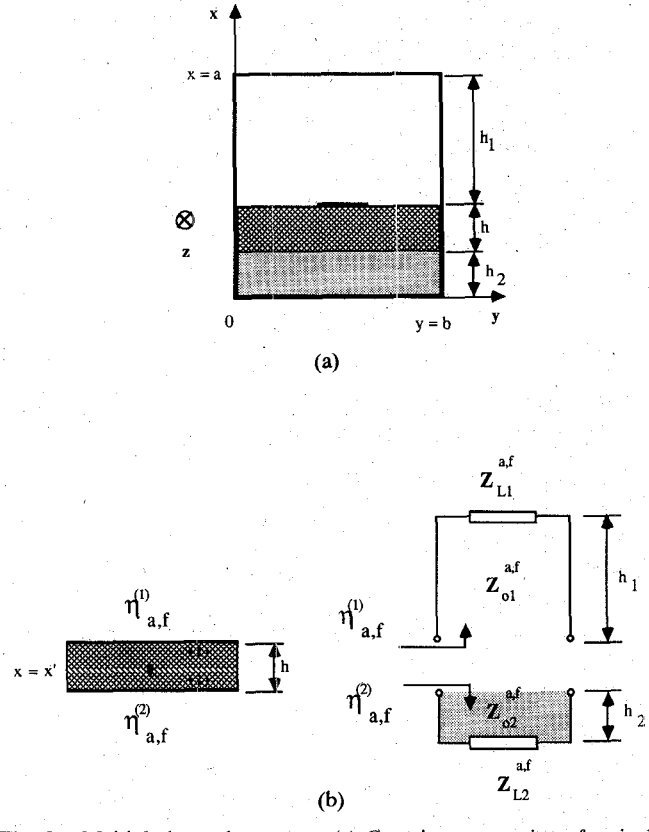

Fig. 2. Multiple layered structure. (a) Generic cross section of a single shielded line. (b) Equivalent geometry containing impedance boundaries.

A. Integral Equation Formulation in the Dielectric Region

The electric field excited by an electric current source depends upon the surface current density $\boldsymbol{J}$ as follows:

$$\boldsymbol{E}(\boldsymbol{r}) = \iint \bar{\bar{G}}(\boldsymbol{r}/\boldsymbol{r}') \cdot \boldsymbol{J}(\boldsymbol{r}')\, ds' \qquad (1)$$

where $\bar{\bar{G}}$ represents the dyadic Green's function in the dielectric regions. The Green's function is derived by evaluating the electric field due to a two-dimensional infinitesimal current source $\boldsymbol{J}(\boldsymbol{r}') = (\hat{y} + \hat{z})\delta(\boldsymbol{r} - \boldsymbol{r}')$, where $\boldsymbol{r}'$ is the position vector of the source. Because of the existence of air and dielectric interfaces, shielded microstrip lines propagate hybrid modes. Determination of these hybrid fields is facilitated by the use of magnetic and electric vector potentials having components in the direction perpendicular to the interfaces, i.e., the x direction [12], [13].

For the case of two-dimensional interconnects, the problem is uniform in the z direction and the Green's function can therefore be solved in the transformed k_z space. The spectral dyadic Green's function $\bar{\bar{G}}$ is obtained by solving the boundary-value problem of the structure under study [14].

In the present derivation, for the sake of clarity, the simple geometry illustrated in Fig. 2 is studied. However, the Green's function is formulated in a generalized way, which can be applied to more complicated problems. The equivalent structure containing impedance boundaries is shown in Fig. 2(b), where the current is displaced from the

interface to generalize the problem and to ease the application of the boundary conditions. The impedance boundaries on the upper and lower interfaces are determined by the use of a single transmission line problem. This formalism has been applied extensively in the past to open structures [15]. The boundary conditions at the upper ($i=1$) and lower ($i=2$) interfaces can be solved separately for LSE (subscript a) and LSM (subscript f) modes. The impedance $\eta^i_{a,f}$ is equivalent to the impedance of a transmission line terminated by a load impedance $Z^{a,f}_{Li}$ with characteristic impedance $Z^{a,f}_{0i}$. The load impedance $Z^{a,f}_{Li}$ may be a lumped impedance, such as the surface resistance of the ground plane, as suggested in Fig. 2(b), or it may be the impedance presented by another substrate layer. The characteristic impedance $Z^{a,f}_{0i}$ is given by the appropriate TM and TE wave impedances.

Inside the equivalent structure, the homogeneous scalar wave equations for A_x and F_x have to be solved in regions (1) ($x>x'$) and (2) ($x<x'$). Applying the method of separation of variables, the following boundary conditions need to be satisfied: (i) vanishing electric fields on the sidewalls, (ii) impedance boundaries on the upper and lower walls as

$$\left(\frac{\tilde{E}_y}{\tilde{H}_z}\right)^i_{a,f} = \eta^i_{a,f} \tag{2}$$

(iii) continuity of the electric fields at $x=x'$, and (iv) discontinuity of the magnetic field components due to the infinitesimal two-dimensional current source at $x=x'$:

$$\hat{n}\times(\tilde{\boldsymbol{H}}^{(1)}-\tilde{\boldsymbol{H}}^{(2)}) = (\hat{y}+\hat{z})\delta(y-y')e^{jk_z z'}|_{x=x'}. \tag{3}$$

Because the current sources are assumed to have both longitudinal and transverse components, four out of six components of the dyadic Green's function are needed.

A more general current distribution $\boldsymbol{J}$ may be written in the form

$$\boldsymbol{J}(\boldsymbol{r}') = \delta(x-x')\boldsymbol{j}(y')e^{-jk_z^{\mathrm{MS}}z'} \tag{4}$$

where k_z^{MS} is the unknown propagation constant of the microstrip. In view of (4), the integral equation for the electric field (1) can be expressed as

$$\boldsymbol{E}(\boldsymbol{r}) = \iint_S \bar{\bar{g}}(x, y/x', y')e^{-jk_z(z-z')}\cdot\boldsymbol{j}(y')e^{-jk_z^{\mathrm{MS}}z'}\,dy'\,dz' \tag{5}$$

where S is the surface of the strip conductors. In the above, the z dependence of both the Green's function and the current is shown explicitly.

Introducing the spectral form of the Green's function $\tilde{\tilde{g}}$, and using the sifting property of the Fourier transform, the electric field can be evaluated at any transverse cross section as

$$\boldsymbol{E} = \int_{C_w} \tilde{\tilde{g}}(x, y/x', y')\cdot\boldsymbol{j}(y')\,dy'|_{k_z=k_z^{\mathrm{MS}}} \tag{6}$$

where C_w is a path along the width of the conductor [14].

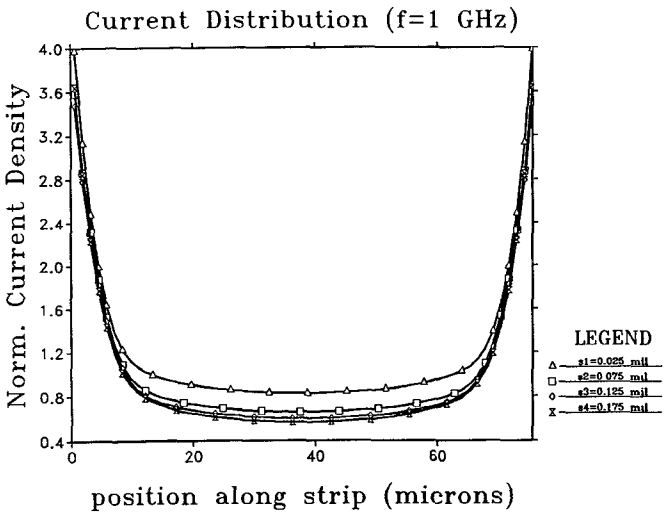

Fig. 3. Magnitude of current density inside a rectangular strip at a height of 3 mils above a perfectly conducting ground ($W=3$ mils, $\sigma=4\times10^7$ S/m, $f=1$ GHz, $t=0.2$ mils).

The above expression satisfies all boundary conditions except the ones on the surface of the strip conductors. For perfectly conducting strips we enforce the Dirichlet condition of vanishing tangential electric field on the surface of the line. This boundary condition is applied to (6), which will be satisfied for discrete values of k_z^{MS} corresponding to the dominant mode and possibly to higher order modes propagating in the structure. For the general case of strips with finite thickness and finite conductivity, this condition is no longer applicable. Indeed, due to the finite conductivity, the fields penetrate inside the strips. An exact analysis of this case requires Maxwell's equations to be solved throughout the entire domain, i.e., in the dielectric regions and inside the lossy strips. Such an analysis is very involved and will not be undertaken here. Instead, we shall follow an alternative, approximate method based on an equivalent representation of the lossy strips by impedance surfaces. These equivalent surfaces are characterized by frequency-dependent surface impedances which are derived from a quasi-TEM analysis of the field penetration and the resulting current distributions inside the lossy strips. The derivation of these impedances is discussed next.

B. Derivation of the Equivalent Surface Impedance

Under the assumption that the transverse component of the current is negligible compared to the longitudinal component, this method is valid through the millimeter-wave frequency range. In this study the current density in the lossy strips of Fig. 1 has the longitudinal component only. An integral equation formulation for the frequency-dependent current distributions in the lossy strips is then possible. The derivation of the pertinent integral equation along with its numerical solution has been presented in [16] and [17] and will not be repeated here. Fig. 3 illustrates the results of this formulation by showing the magnitude of the current density along the width of the strip,

plotted for four different distances s_1, s_2, s_3, and s_4 from the bottom side of the strip.

Once the current distributions have been computed, the per-unit-length resistance $R(f)$ and inductance $L(f)$ of the lossy strips can be found from energy considerations as described in [17]. The per-unit-length internal inductance of the strip is then computed as

$$L_{\text{in}}(f) = L(f) - L_{\infty} \tag{7}$$

where L_{∞} is the per-unit-length inductance of the strip in the limit $\sigma \to \infty$, in which case the current flows on the surface of the strip and there is no field penetration. Knowledge of the per-unit-length strip resistance and internal inductance allows us to express the per-unit-length voltage drop ΔV along the lossy strip as

$$-\Delta V = [R(f) + j2\pi f L_{\text{in}}(f)]I \quad \text{(V/m)} \tag{8}$$

where I is the total current flowing in the strip.

In order to derive the desirable surface impedance, we start with the standard definition for the surface impedance of an imperfect conductor as the ratio of the tangential component of the electric field to the surface current density at the conductor surface:

$$E_z(\tau) = Z(\tau)J_{zs}(\tau) = Z(\tau)H_y(\tau) \tag{9}$$

where τ is the transverse coordinate along the surface of the conductor. Integrating (9) along the side of the strip, we have

$$\int_0^W E_z(\tau)\,d\tau = \int_0^W Z(\tau)H_y(\tau)\,d\tau \tag{10}$$

where W is the width of the strip. From (10) using the mean value theorem for Riemann integration [18] we can write

$$\int_0^W E_z(\tau)\,d\tau = Z(\tau_0)\int_0^W H_y(\tau)\,d\tau \tag{11}$$

where $\tau_0 \in [0,W]$. Dividing both sides of (11) by W and recognizing the integral on the right-hand side as the total current flowing on the surface, we can write

$$\tilde{E}_z = Z(\tau_0)\frac{I}{W} \tag{12}$$

where $\tilde{E}_z$ is the average value of the longitudinal component of the electric field on the strip. Obviously, this value can be thought of as the negative of the per-unit-length average voltage drop along the strip, in which case (8) and (12) lead to the relation

$$Z(\tau_0) = W[R(f) + j\omega L_{\text{in}}(f)]. \tag{13}$$

This is the desirable expression for the surface impedance of the equivalent impedance surface to be used in place of the lossy strip. In what follows, we shall denote this surface impedance as $Z_l(f)$ where the subscript l suggests its relation to the longitudinal current on the strip. A transverse component of the current also exists, and a transverse surface impedance Z_t can be defined as discussed in the following section.

C. Application of Boundary Condition

The electric and magnetic fields tangential to the surface of the strips are related through the surface impedance derived in the previous section as

$$\frac{E_z}{H_y} \equiv Z_l(f). \tag{14}$$

For most practical purposes, the dominant part of the conductor loss is due to the longitudinal component of the current, for which the accurate longitudinal surface impedance $Z_l(f)$ has been proposed. However, as the frequency of interest becomes higher and/or the width of the strip increases, the transverse component of the current becomes more significant and needs to be accounted for. This is being done using the standard surface impedance for an infinite resistive plane as

$$-\frac{E_y}{H_z} \equiv Z_t = (1+j)\frac{1}{\sigma\delta} \tag{15}$$

where σ is the conductivity of the strip and δ the skin depth at the frequency of interest. Even if the width of the strip is finite, use of (15) is justified by the fact that the strip is assumed to be infinite in the direction perpendicular to the flow of the transverse component of the current.

In view of (14) and (15), equation (6) takes the form

$$\boldsymbol{E} = \int_{C_w} \tilde{\bar{g}}(x, y/x', y')\cdot\boldsymbol{j}(y')\,dy' + \bar{\bar{Z}}\cdot(\boldsymbol{H}\times\hat{n})|_{k_z=k_z^{\text{MS}}} \tag{16}$$

where $\bar{\bar{Z}}$, a dyadic quantity that we call the *dyadic surface impedance*, is given by

$$\bar{\bar{Z}} = Z_t\hat{y}\hat{y} + Z_l\hat{z}\hat{z}. \tag{17}$$

Recognizing the boundary condition for the magnetic field as

$$\hat{n}\times\boldsymbol{H} = \boldsymbol{J} \tag{18}$$

(16) becomes

$$\int_{C_w} g \cong (x, y/x', y')\cdot\boldsymbol{j}(y')\,dy' - \bar{\bar{Z}}\cdot\boldsymbol{j}(y')|_{k_z=k_z^{\text{MS}}} = 0. \tag{19}$$

The method of moments is adopted here to solve for the current distribution. The two-dimensional surface current may be written as

$$\boldsymbol{j}(y') = j_y(y')\hat{y} + j_z(y')\hat{z} \tag{20}$$

where $j_y(y')$ and $j_z(y')$ are unknown functions of y'. Entire domain basis functions are chosen to approximate the behavior of the current distribution. The longitudinal current is represented by Chebyshev polynomials of the first kind T_i, and the transverse current is approximated by Chebyshev polynomials of the second kind U_i. These basis functions are multiplied by their respective weighting functions in order to satisfy the edge conditions

$$j_y(y') = \sum_{p=1}^{P} I_{yp} U_p\left(\frac{2}{W}(y'-y_0)\right)\sqrt{1-\left(\frac{2}{W}(y'-y_0)^2\right)} \tag{21}$$

$$j_z(y') = \sum_{q=0}^{P-1} I_{zq} \frac{T_q\left(\frac{2}{W}(y'-y_0)\right)}{\sqrt{1-\left(\frac{2}{W}(y'-y_0)^2\right)}}. \tag{22}$$

In the above expressions W is the width of the strip and y_0 is the distance from the origin to the center of the strip. Introducing these expressions for the basis functions, (19) results in closed-form integrals that simplify to Bessel functions of integer order.

The testing functions are chosen as Chebyshev polynomials of the form

$$w_p^y(y) = U_p\left(\frac{2}{W}(y-y_0)\right) \tag{23}$$

$$w_q^z(y) = T_q\left(\frac{2}{W}(y-y_0)\right). \tag{24}$$

This method is a variation of Galerkin's procedure. The integrals resulting from the weighted averages are expressed in terms of spherical Bessel functions. This technique results in a homogeneous system of simultaneous algebraic equations which can be solved by setting the determinant of the impedance matrix $[\mathscr{Z}]$ equal to zero. Expressions for the elements of $[\mathscr{Z}]$ are given in the Appendix. The roots of the determinant correspond to the propagation constants of the excited modes.

III. Numerical Results

Based on the theory presented in the previous section, the complex propagation constant in high-frequency interconnects is evaluated as a function of various parameters by using Muller's algorithm with deflation. Each element of this matrix involves a summation over the modes of the inhomogeneously filled waveguide along the y direction. The number of modes considered is enough to ensure convergence.

As it has been discussed by many authors, isolated microstrip interconnects can propagate a dominant mode with zero cutoff frequency and higher order modes which are in one-to-one correspondence with the modes of the inhomogeneously filled waveguide surrounding them. All these modes are hybrid in nature and exhibit strong dependence on the electrical and geometrical characteristics of the microstrip interconnects and the shielding structure. From the parameters which affect the characteristics of the propagating modes, the strip width W to substrate thickness ratio (aspect ratio) and the operating frequency are the most important ones. This paper gives an extensive parametric study of the attenuation of the dominant mode and the derived results are compared with available data whenever possible.

In Fig. 4, conductor and dielectric losses calculated with the present technique are shown as a function of the aspect ratio. For thick strips, results derived in this paper are compared with the finite element method (FEM) [6], the spectral-domain method (SDM) [7], [19] and an analytic differentiation of Wheeler's *incremental inductance rule* [2].[1] All the existing full-wave analysis models evaluate conductor losses by using a perturbation method where the surface resistivity is given by the incremental inductance rule and, as a result, cannot predict losses for conducting strips with thickness of the order of a skin depth. The effect of the conductor strip thickness on conductor losses is explicitly shown on Fig. 5. On the figure, conductor losses versus aspect ratio are plotted for the case of $t = 0.5\delta$, which appear substantially different from the case of $t = 2$, 3, and 4δ (electrically thick strips). Our results correctly predict that as the thickness of the strip increases to values large compared to the skin depth, the loss decreases significantly to the thick strip limit. This, of course, is due to the fact that the current is forced to flow through a smaller area.

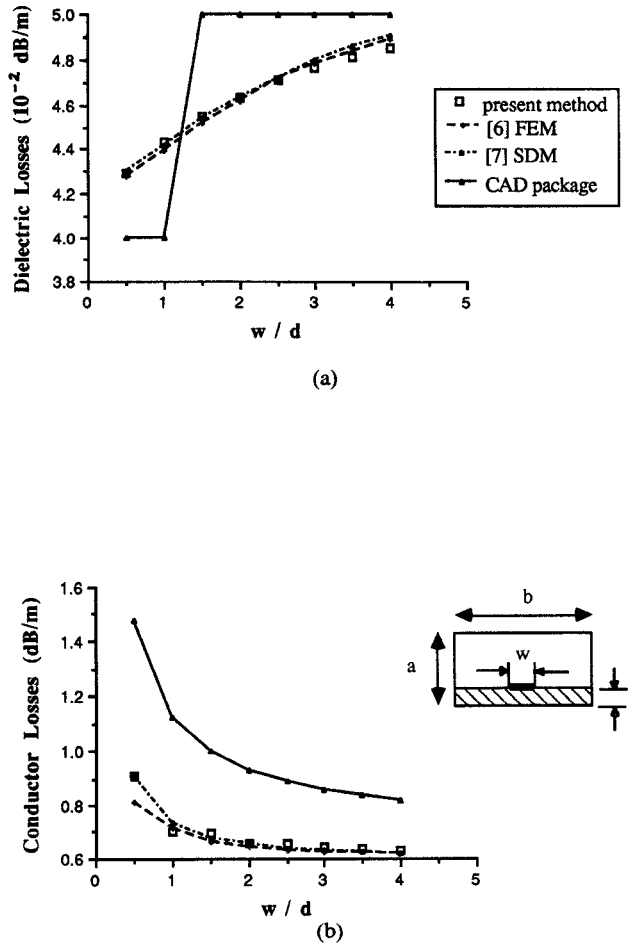

Fig. 4. Conductor and dielectric losses of a single strip versus strip width ($a = 10$ mm, $b = 20$ mm, $d = 1$ mm, $\epsilon_r = 10$, $\delta = 3.33 \times 10^7$ S/m, $\tan\delta = 2 \times 10^{-4}$, $f = 1$ GHz, $t = 0.01$ mm). (a) Dielectric attenuation as a function of w/d. (b) Ohmic attenuation as a function of w/d.

[1]This analytic differentiation is implemented through the microwave CAD software package LineCalc, available from EESOF.

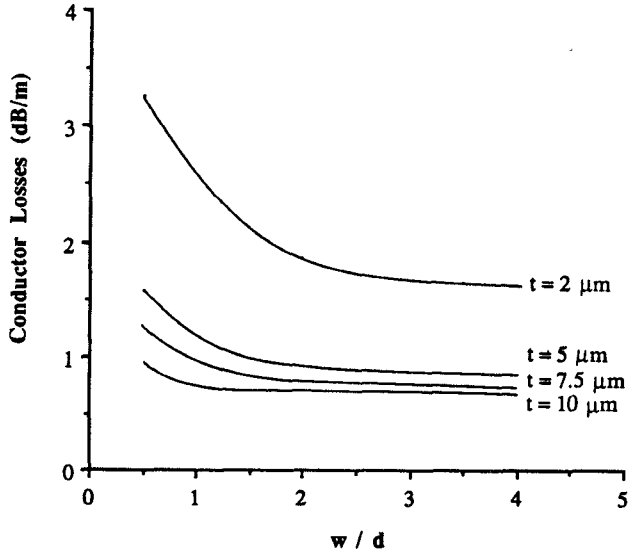

Fig. 5. Effect of thickness on the ohmic attenuation constant ($a = 10$ mm, $b = 20$ mm, $d = 1$ mm, $\epsilon_r = 10$, $\sigma = 3.33 \times 10^7$ S/m, $f = 1$ GHz).

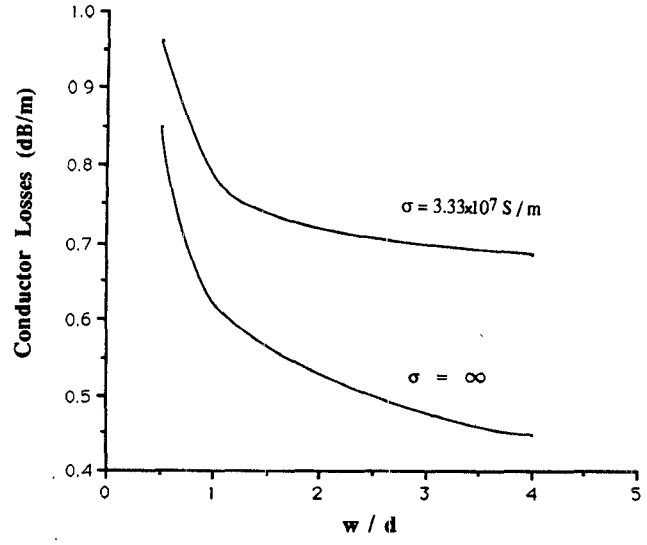

Fig. 7. Effect of ground plane resistivity on the ohmic attenuation constant ($a = 10$ mm, $b = 20$ mm, $d = 1$ mm, $\epsilon_r = 10$, $\sigma = 3.33 \times 10^7$ S/m, $f = 1$ GHz).

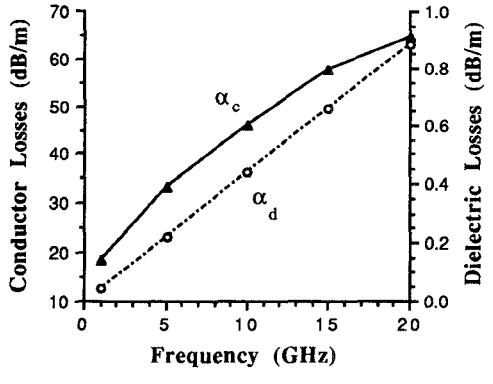

(a)

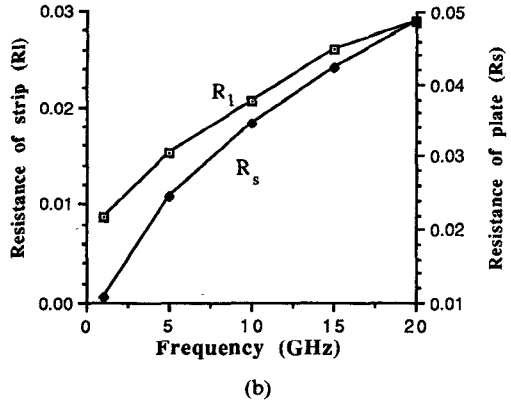

(b)

Fig. 6. Effect of frequency on the attenuation constant ($a = b = 500$ μm, $W = d = 50$ μm, $\epsilon_r = 10$, $\sigma = 3.33 \times 10^7$ S/m, $t = 5$ μm). (a) Dielectric and conductor losses versus frequency. (b) Equivalent surface resistivity R_l and ground resistivity R_s versus frequency.

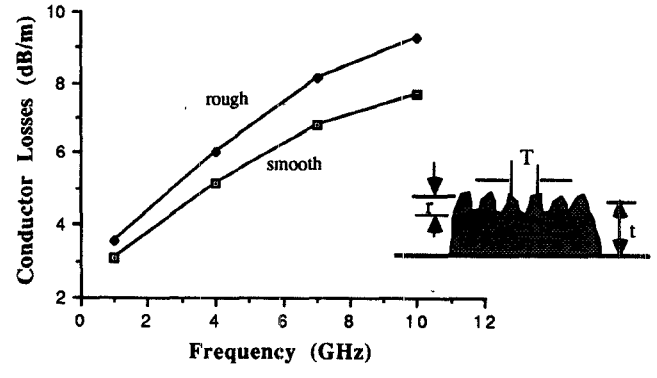

Fig. 8. Effect of roughness on the ohmic attenuation constant as a function of frequency ($a = 10$ mm, $b = 20$ mm, $W = d = 280$ μm, $T = 70$ μm, $r = 1.5$ μm, $\epsilon_r = 10$, $\sigma = 4 \times 10^7$ S/m, $t = 6$ μm).

The skin-effect problem may also be described as a function of frequency. The attenuation constant α is plotted in Fig. 6 for frequencies up to 20 GHz. Also shown are the equivalent surface resistance of the strip (eq. (13)) and the surface resistivity R_s of the infinite thick plane representing the ground plane resistance. By using R_s as the surface resistivity of the ground plane, results have been derived which show the effect of the lossy ground on conductor losses (see Fig. 7). This effect is very important and therefore losses due to ground plane cannot be neglected.

The present method also allows to account accurately for multiple metallizations and roughness of the surface of the strip conductors. In Fig. 8, the effect of a periodic variation of the surface roughness on conductor losses is plotted as a function of frequency.

The technique presented in this paper has also been applied to evaluate conductor and dielectric losses for the even and odd excitation modes in the case of two edge-coupled electrically thick strips. The derived results are plotted in Fig. 9 as a function of the separation between

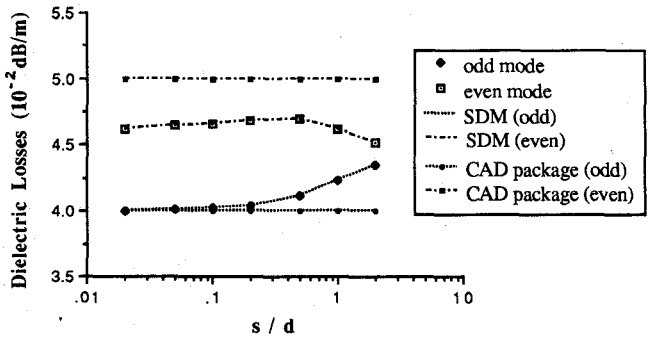

(a)

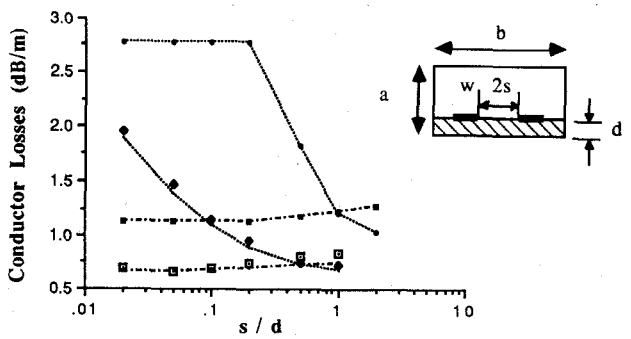

(b)

Fig. 9. Conductor and dielectric losses of coupled strips versus line separation ($a=10$ mm, $b=20$ mm, $W/d=1$, $\epsilon_r=10$, $\sigma=3.33\times10^7$ S/m, $\tan\delta=2\times10^{-4}$, $f=1$ GHz, $t=0.01$ mm). (a) Dielectric attenuation as a function of s/d. (b) Ohmic attenuation as a function of s/d.

the two strips and are compared to results derived with the spectral-domain method [7], [19]. The agreement is very good. Similar results are presented in Fig. 10 for the case of two-level interconnects as a function of frequency.

IV. Summary

An integral equation method has been applied to calculate the propagation constant in shielded multilayer structures involving an arbitrary number of non-perfectly conducting strips by using the combination of a static Green's function inside the strips and a hybrid Green's function formulation in the dielectrics. This method allows for the evaluation of dielectric losses in the substrate layers and conductor losses in strips of arbitrary thickness. The skin-effect problem is addressed and results show an increase in the attenuation constant for thin strips. As expected, finite conductive ground plane and roughness of the strip increase the attenuation constant substantially. Several interconnect structures are analyzed, such as single lines and edge-coupled and broadside-coupled strips, and they compare well with available data.

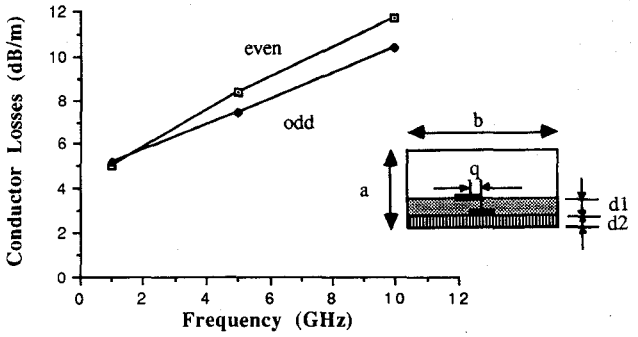

Fig. 10. Ohmic losses of two-layer interconnects versus frequency ($a=1$ mm, $b=2$ mm, $d_1=0.2$ mm, $d_2=0.1$ mm, $q=0.5$ mm, $\epsilon_{r1}=4$, $\epsilon_{r2}=1$, $\sigma=3.33\times10^7$ S/m, $t=4$ μm).

Appendix
Expressions for the Elements of the Impedance Matrix $\mathscr{Z}$

$$\left(\mathscr{Z}_{yy}^{qp}\right)^i=\frac{2}{b}j\omega\mu_0\sum_m-\frac{1}{k_y^2+k_z^2}\left\{\frac{k_z^2}{k_{xr}}\left(\varphi_m^f\right)^i+\frac{k_y^2k_{xr}}{k_r^2}\left(\varphi_m^a\right)^i\right\}\cdot\mathscr{I}_q^{(4)}\mathscr{I}_p^{(2)}-Z_l\mathscr{I}_{qp}^{(6)} \tag{A1}$$

$$\left(\mathscr{Z}_{yz}^{qp}\right)^i=\frac{2}{b}\omega\mu_0\sum_m\frac{k_yk_z}{k_y^2+k_z^2}\left\{-\frac{1}{k_{xr}}\left(\varphi_m^f\right)^i+\frac{k_{xr}}{k_r^2}\left(\varphi_m^a\right)^i\right\}\cdot\mathscr{I}_q^{(4)}\mathscr{I}_p^{(1)} \tag{A2}$$

$$\left(\mathscr{Z}_{zy}^{qp}\right)^i=\frac{2}{b}\omega\mu_0\sum_m\frac{k_yk_z}{k_y^2+k_z^2}\left\{-\frac{1}{k_{xr}}\left(\varphi_m^f\right)^i+\frac{k_{xr}}{k_r^2}\left(\varphi_m^a\right)^i\right\}\cdot\mathscr{I}_q^{(3)}\mathscr{I}_p^{(2)} \tag{A3}$$

$$\left(\mathscr{Z}_{zz}^{qp}\right)^i=\frac{2}{b}j\omega\mu_0\sum_m\frac{1}{k_y^2+k_z^2}\left\{\frac{k_y^2}{k_{xr}}\left(\varphi_m^f\right)^i+\frac{k_z^2k_{xr}}{k_r^2}\left(\varphi_m^a\right)^i\right\}\cdot\mathscr{I}_q^{(3)}\mathscr{I}_p^{(1)}-Z_l\mathscr{I}_{qp}^{(5)} \tag{A4}$$

where

$$k_r=\omega\sqrt{\epsilon_r^*\mu_0} \tag{A5}$$

$$k_y=\frac{m\pi}{b} \tag{A6}$$

$$k_{xr}=\sqrt{(k_r)^2-k_y^2-k_z^2} \tag{A7}$$

and

$$\left(\varphi_m^{a,f}\right)^1=-\frac{\dfrac{\cos k_{xr}(x-h)}{\cos k_{xr}(x'-h)}\dfrac{\tan k_{xr}(x-h)+j\eta_{a,f}^1}{1-j\eta_{a,f}^2\tan k_{xr}x'}}{\dfrac{\tan k_{xr}(x'-h)+j\eta_{a,f}^1}{\tan k_{xr}x'+j\eta_{a,f}^2}-\dfrac{-1-j\eta_{a,f}^1\tan k_{xr}(x'-h)}{1-j\eta_{a,f}^2\tan k_{xr}x'}} \tag{A8}$$

$$\left(\varphi_m^{a,f}\right)^2 = \frac{\dfrac{\cos k_{xr}x}{\cos k_{xr}x'}\dfrac{\tan k_{xr}x + j\eta_{a,f}^2}{1 - j\eta_{a,f}^1 \tan k_{xr}(x'-h)}}{\dfrac{\tan k_{xr}x' + j\eta_{a,f}^2}{\tan k_{xr}(x'-h) + j\eta_{a,f}^1} - \dfrac{1 - j\eta_{a,f}^2 \tan k_{xr}x'}{1 - j\eta_{a,f}^1 \tan k_{xr}(x'-h)}} \tag{A9}$$

In (A5), ϵ_r^* is the complex permittivity of the substrate, and i ($=1, 2$) represents the regions above and below the point source, respectively.

Further definitions necessary for the interpretation of (A1)–(A4) are provided as

$$\mathcal{I}_n^{(1)} = \frac{W}{2}\pi \sin\left(k_y y_0 + n\frac{\pi}{2}\right) J_n\left(k_y \frac{W}{2}\right) \tag{A10}$$

$$\mathcal{I}_n^{(2)} = \frac{\pi}{k_y}(n+1)\cos\left(k_y y_0 + n\frac{\pi}{2}\right) J_{n+1}\left(k_y \frac{W}{2}\right) \tag{A11}$$

$$\mathcal{I}^{(5)} = \begin{cases} W\frac{\pi}{2} & \text{for } m = n = 0 \\ W\frac{\pi}{4} & \text{for } m = n \neq 0 \\ 0 & \text{for } m \neq n \end{cases} \tag{A12}$$

and

$$\mathcal{I}^{(6)} = \begin{cases} W\dfrac{\pi}{4} & \text{for } m = n \\ 0 & \text{for } m \neq n. \end{cases} \tag{A13}$$

No general recurrence formulas were found for $\mathcal{I}^{(3)}$ and $\mathcal{I}^{(4)}$. However, these integrals can be written in a simple form as a weighted sum of spherical Bessel functions.

In equations (A8) and (A9), η_a^i and η_f^i are given by

$$\eta_a^i = \frac{\omega\epsilon_r^*}{k_{xr}} Z_{0i}^a \frac{Z_{Li}^a + jZ_{0i}^a \tan k_{x_i}h_i}{Z_{0i}^a + jZ_{Li}^a \tan k_{x_i}h_i} \tag{A14}$$

$$\eta_f^i = \frac{k_{xr}}{\omega\mu_0} Z_{0i}^f \frac{Z_{Li}^f + jZ_{0i}^f \tan k_{x_i}h_i}{Z_{0i}^f + jZ_{Li}^f \tan k_{x_i}h_i} \tag{A15}$$

where

$$Z_{0i}^f = \frac{\omega\mu_0}{k_{xi}} \tag{A16}$$

$$Z_{0i}^a = \frac{k_{xi}}{\omega\epsilon_i^*}. \tag{A17}$$

REFERENCES

[1] H. A. Wheeler, "Formulas for the skin effect," *Proc. IRE*, vol. 30, pp. 412–424, Sept. 1942.

[2] R. A. Pucel, D. J. Masse, and C. P. Hartwig, "Losses in microstrip," *IEEE Trans. Microwave Theory Tech.*, vol. MTT-16, pp. 342–350, June 1968.

[3] M. V. Schneider, "Microstrip lines for microwave integrated circuits," *Bell Syst. Tech. J.*, pp. 1421–1444, May–June 1969.

[4] H. A. Wheeler, "Transmission-line properties of a strip on a dielectric sheet on a plane," *IEEE Trans, Microwave Theory Tech.*, vol. MTT-25, pp. 631–647, Aug. 1977.

[5] B. E. Spielman, "Dissipation loss effects in isolated and coupled transmission lines," *IEEE Trans. Microwave Theory Tech.*, vol. MTT-25, pp. 648–655, Aug. 1977.

[6] Z. Pantic-Tanner and R. Mittra, "Finite-element matrices for loss calculation in quasi-TEM analysis of microwave transmission lines," *Microwave and Opt. Technol. Lett.*, vol. 1, no. 4, pp. 142–146, June 1988.

[7] D. Mirshekar-Syahkal and J. B. Davies, "Accurate solution of microstrip and coplanar structures for dispersion and for dielectric and conductor losses," *IEEE Trans. Microwave Theory Tech.*, vol. MTT-27, pp. 694–699, July 1979.

[8] C. M. Crowne, "Microstrip conductor losses calculated by full wave and perturbational approaches," *Electron. Lett.*, vol. 24, no. 9, pp. 552–553, Apr. 1988.

[9] R. H. Jansen, "High speed computation of single and coupled microstrip parameters including dispersion, high-order modes, loss and finite strip thickness," *IEEE Trans. Microwave Theory Tech.*, vol. MTT-26, pp. 75–82, Feb. 1978.

[10] P. Waldow and I. Wolff, "The skin-effect at high frequencies," *IEEE Trans. Microwave Theory Tech.*, vol. MTT-33, pp. 1076–1082, Oct. 1985.

[11] G. I. Costache, "Finite element method applied to skin-effect problems in strip transmission lines," *IEEE Trans. Microwave Theory Tech.*, vol. MTT-35, pp. 1009–1013, Nov. 1987.

[12] N. K. Das and D. M. Pozar, "A generalized spectral-domain Green's function for multilayer dielectric substrates with application to multilayer transmission lines," *IEEE Trans. Microwave Theory Tech.*, vol. MTT-35, pp. 326–335, Mar. 1987.

[13] T. G. Livernois and P. B. Katehi, "A generalized method for deriving the space-domain Green's function in a shielded, multilayer substrate structure with applications to MIS slow-wave transmission lines," *IEEE Trans. Microwave Theory Tech.*, vol. 37, pp. 1761–1767, Nov. 1989.

[14] T. E. van Deventer and P. B. Katehi, "Conductor losses in high frequency interconnects," Radiation Laboratory Rep., University of Michigan, in preparation.

[15] L. Beyne and D. de Zutter, "Green's function for layered lossy media with special application to microstrip antennas," *IEEE Trans. Microwave Theory Tech.*, vol. 36, pp. 875–881, May 1988.

[16] A. C. Cangellaris, "The importance of skin-effect in microstrip lines at high frequencies," in *IEEE MTT-S Int. Microwave Symp. Dig.*, May 1988, pp. 197–198.

[17] A. C. Cangellaris, J. L. Prince, and O. A. Palusinski, "Modeling of high-speed interconnects; An integral equation approach to inductance computation," in *Proc. 1988 Summer Computer Simul. Conf.*, July 1988, pp. 33–36.

[18] E. T. Whittaker and G. N. Watson, *A Course of Modern Analysis*, London: Cambridge University Press, 1927, pp. 65–66.

[19] D. Mirshekar-Syahkal, "An accurate determination of dielectric loss effect in monolithic microwave integrated circuits including microstrip and coupled microstrip lines," *IEEE Trans. Microwave Theory Tech.*, vol. MTT-31, pp. 950–954, Nov. 1983.

✠

T. Emilie van Deventer (S'87) was born in Hillerød, Denmark, on October 3, 1961. She received the Diplome Universitaire de Technologie from the Institut Universitaire de Technologie (I. U. T.), Marseille, France, in 1982, and the B.S.E. and M.S.E. degrees in electical engineering from the University of Michigan, Ann Arbor, in 1985 and 1986 respectively. She is currently working toward the Ph.D. degree on the subject of numerical modeling of microwave and millimeter-wave structures.

She worked in the acoustic field for Bruel & Kjaer from 1982 to 1983. In 1985 she joined the Radiation Laboratory at the University of Michigan as a research assistant, where she studied scattering and attenuation by nonlinear media. She is a member of the IEEE MTT-S and AP-S, Tau Beta Pi, and Eta Kappa Nu.

Pisti B. Katehi (S'81–M'84–SM'89) received the B.S.E.E. degree from the National Technical University of Athens, Greece, in 1977 and the M.S.E.E. and PhD. degrees from the University of California, Los Angeles, in 1981 and 1984 respectively.

In September 1984 she joined the faculty of the EECS Department of the University of Michigan, Ann Arbor, as an Assistant Professor. Since then, she has been involved in the modeling and computer-aided design of millimeter-wave and near-millimeter-wave monolithic circuits and antennas.

In 1984 Dr. Katehi received the W. P. King Award and in 1985 the S. A. Schelkunoff Award from the Antennas and Propagation Society. In 1987 she received an NSF Presidential Young Investigator Award and a Young Scientist Fellowship awarded from URSI. Dr. Katehi is a member of IEEE AP-S, MTT-S and Sigma Xi.

Andreas C. Cangellaris (M'86) received the Diploma in electrical engineering from the Aristotellan University of Thessaloniki, Greece, in 1981, and the M.S. and Ph.D. degrees from the University of California, Berkeley, in 1983 and 1985, respectively, both in electrical engineering.

From 1985 to 1987, he was with the Electrical and Electronics Engineering Department, General Motors Research Laboratories, Warren, Michigan. Since 1987 he has been an Assistant Professor with the Department of Electrical and Computer Engineering, University of Arizona, Tucson, where he teaches graduate and undergraduate courses on electromagnetic theory, microwave circuits, and computational methods in electromagnetics. His research interests are in numerical methods for electromagnetic wave scattering and propagation, analysis of microwave integrated circuits, and electromagnetic characterization of high-speed interconnections for VLSI packages.